Research on Power of Resonant Wireless Power Transfer System at Different Distances

Jianliang Li[1, a,*], TingChuan Xie[1], Jing Kang[1], Yalan Hao[2], Qiuyue Zhang[1], Yuefei Ma[1]

[1] School of Construction Machinery College, Chang'an University, Xi'an 710064, China.

[2] School of Highway, Chang'an University, Xi'an 710064, China.

*, a 414777192@qq.com

Abstract. Resonant Wireless Power Transfer (RWPT) is free from wired transmission. It has also realized long-distance power transmission, which has become one of the hotspots at home and abroad. Based on the existing research foundation, this paper focuses on the analysis of the inverter module, rectifier module and resonant coupling module from the components of RWPT. Further, PSpice simulation is used to analyze the IR2110 driving circuit and the transmission process of the whole system. Finally, a RWPT system is set up to explore the feasibility and effectiveness of theoretical analysis and practical experiments.

Key words: RWPT; PSpice; IR2110.

1. Rwpt System Introduction

The discovery of RWPT can be traced back to the end of the nineteenth Century, Nicola Tesla did a lot of research on it . Then, MIT's research team really pushed RWPT into the hot spot of scientific research in 2007[1].The components of the RWPT system are shown in FIG 1. Power frequency AC power from the power grid is changed into direct current power by rectifier circuit (AC-DC), direct current power by chopper circuit (DC-DC) and high frequency AC power by inverter circuit (DC-AC). Next, high frequency electricity passes through the resonant circuit to transfer energy from the original side to the secondary side, and the secondary side is then output to the load through the rectification circuit (DC-DC) and the filter circuit [2].
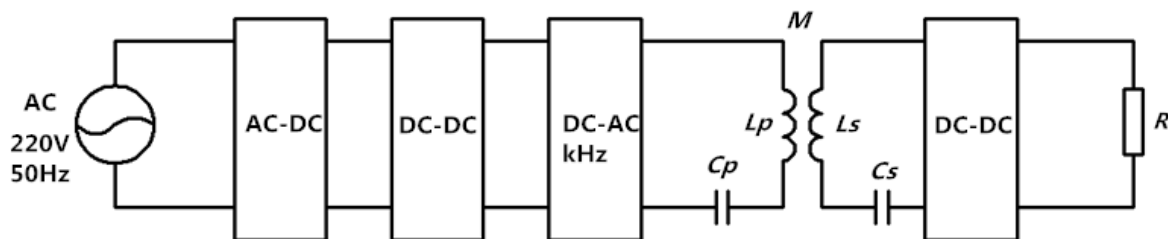

Fig. 1 Electrical Schematic for WP

2. System Analysis

2.1 Module Analysis

In this study, the DC switching power supply is used as the energy transmitting end. Therefore, the original side inverter module, the secondary side rectification filtering module and the resonance module are mainly studied. According to the existing research foundation, the inverter module uses a full-bridge inverter circuit, the rectifier module uses a full-wave uncontrollable rectifier circuit, and the resonance module uses a string-string type resonant circuit [3].
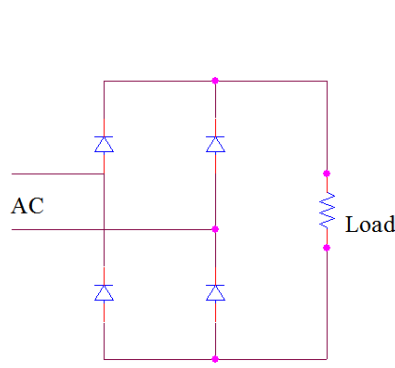
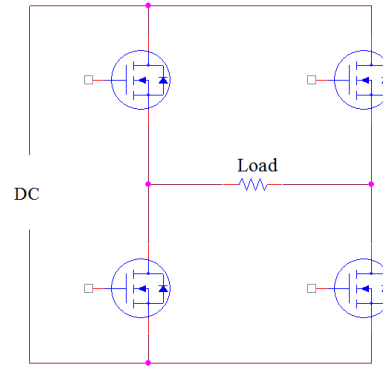Fig. 2 Full Bridge Inverter Circuit   Fig. 3 Full Wave Rectifying Circuit
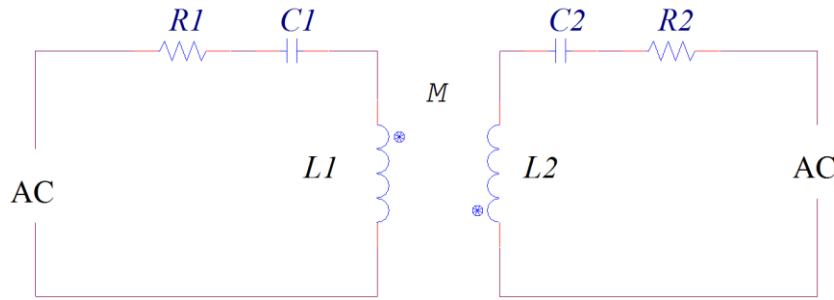

Fig.4 Serial Resonant Circuit

As shown in FIG. 2, the full-bridge inverter circuit is mainly composed of four switching tubes, and the diagonal line is one group, there are two groups in total. Under the control of the driving signal, the two sets of switching tubes are alternately turned on, thereby achieving DC-changing communication.

As shown in FIG 3, the rectifying circuit is mainly composed of four diodes, and the diagonal line is one group, which alternately passes through alternating current, rectifies into direct current, and then supplies power to the load end through a filter voltage stabilizing circuit.

As shown in FIG. 4, the resonant module is a serial resonant circuit, namely LC oscillation circuit. Among them, R1 and R2 are circuit equivalent internal resistance, C1 and C2 are resonant capacitors, L1 and L2 are resonant inductors, M is mutual inductance, and k is a coupling coefficient. The mutual relationship between mutual inductance and coupling coefficient is $M = k\sqrt{L_1 L_2}$ .In the power-on state, L and C produce oscillations. When the frequency of the original and secondary oscillations is the same, the resonance is produced and the resonant frequency is $f = 1/2\pi\sqrt{LC}$. At this time, a larger power of energy transmission can be realized.

The circuit equations of the circuit can be obtained by Kirchhoff's law and mutual inductance theory [4]:

$$\begin{cases} U = Z_1 I_1 - j\omega_1 M I_2 \\ 0 = Z_2 I_2 - j\omega_2 M I_1 \end{cases} \tag{1}$$

U is the power supply voltage. I_1 and I_2 are the currents of the original and secondary sides. ω_1 and ω_2 are the original and secondary resonant angular frequencies. Among them,

$$\begin{cases} Z_1 = R_1 + \dfrac{1}{j\omega_1 C_1} + j\omega_1 L_1 \\ Z_2 = R_2 + R + \dfrac{1}{j\omega_2 C_2} + j\omega_2 L_2 \end{cases} \tag{2}$$

In the resonant state, the resonant frequency of the original and secondary sides is the same. It behaves as $\omega = \omega_1 = \omega_2$. Introduced by the resonant conditions mentioned above (the resonant conditions is $\omega = \dfrac{1}{\sqrt{LC}}$), we deduce $L_1 C_1 = L_2 C_2$, and we know that $\omega L = \dfrac{1}{\omega C}$. Then we can calculate the expression of two unknowns I_1, I_2 in equation (1):

$$I_1 = \frac{U(R_2 + R)}{R_1(R_2 + R) + (\omega M)^2} \tag{3}$$

$$I_2 = \frac{j\omega MU}{R_1(R_2 + R) + (\omega M)^2} \tag{4}$$

The power calculation formula for the load is

$$P = I^2 R \tag{5}$$

Substituting equation (4 into equation (5), the power of the load is

$$P = \frac{(\omega M)^2 U^2 R}{\left[R_1(R_2 + R) + (\omega M)^2 \right]^2} \tag{6}$$

The transmission efficiency of the system is the ratio of load power to power output power, i. e,

$$\eta = \frac{P}{UI_1} = \frac{(\omega M)^2 R}{\left[R_1(R_2 + R) + (\omega M)^2 \right](R_2 + R)} \tag{7}$$

In order to better analyze the influence of coil coupling coefficient on system power and efficiency, the mathematical relationship was explored with software Mathcad. We assume that the power supply voltage is 12V, the inductance is 135uh, the capacitance is 0.47nf, the equivalent resistance is 0.5Ω, and the calculated resonant frequency is 20 kHz. The coupling coefficient K is set to 0.1~1.0 with a step length of 0.01. As shown in FIG. 5, the relationship between the total impedance and the loop current of the series resonant circuit shows that the total impedance at the resonance point is 0.473, and the current value is at most 25.385, which is most beneficial for energy transmission. In addition, it can be seen that the frequency range which can be adjusted is small, and once it deviates from the resonance point, the impedance sharply increases, and the current suddenly drops [5]. FIG. 6 shows the relationship between the coupling coefficient k and efficiency and power, which increases the efficiency by 50 times for analysis. It can be seen that with increasing of the coupling coefficient, the efficiency increase firstly and then stabilizes, and the power increases firstly and then decreases. This provides a reference standard for the next step of selection.
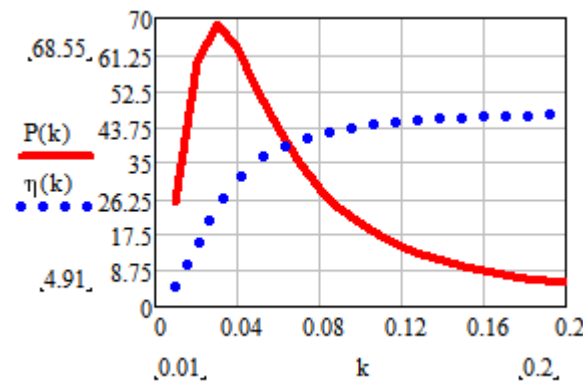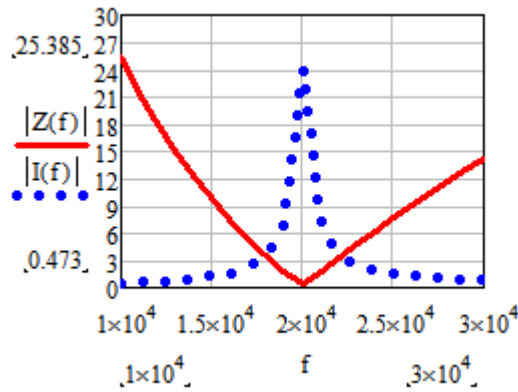

Fig. 5Relationship between Total Impedance and Current

Fig. 6The Relationship between Coupling Coefficient k and Efficiency and Power

2.2 Simulation Analysis

This part is mainly based on the above analysis, using PSpice software to simulate inverter, rectifier and the whole system.

The 12V DC power source is selected as the energy source. According to the related calculation, the inverter circuit switch tube is irf840, the continuous current diode is 1N4376, the drive chip is IR2110, each IR2110 can send 1 high level, 1 low level, and then controls the switch of the MOSFET switch.

According to the analysis of FIG. 5 and FIG. 6, the system has the best effect at the frequency of 20kHz, and the coupling coefficient is best between 0.02~0.08.

In the IR2110 drive circuit of FIG. 7, the switching frequency is set to 20 kHz, which is consistent with the resonant frequency of the coupled part in FIG. 8, and the coupling coefficient is fixed to 0.06, in which the PWM wave uses two pulse power sources to replace the function of the TMS320F28335.

FIG. 9 is the four waveform of the two IR2110, and setting a certain dead time to prevent the short circuit of the inverting circuit from going up and down with the bridge arm.

FIG. 10 and FIG. 11 are the pickup voltage of the secondary coil and the voltage diagram of the load side after being rectified.
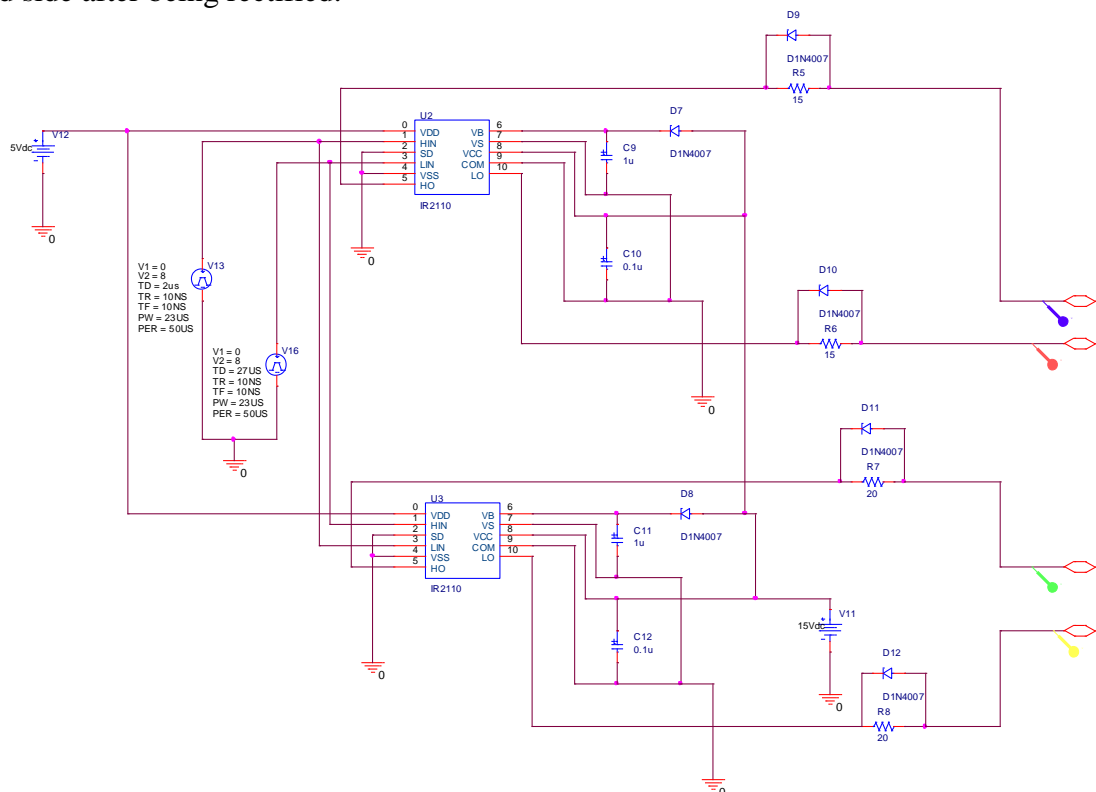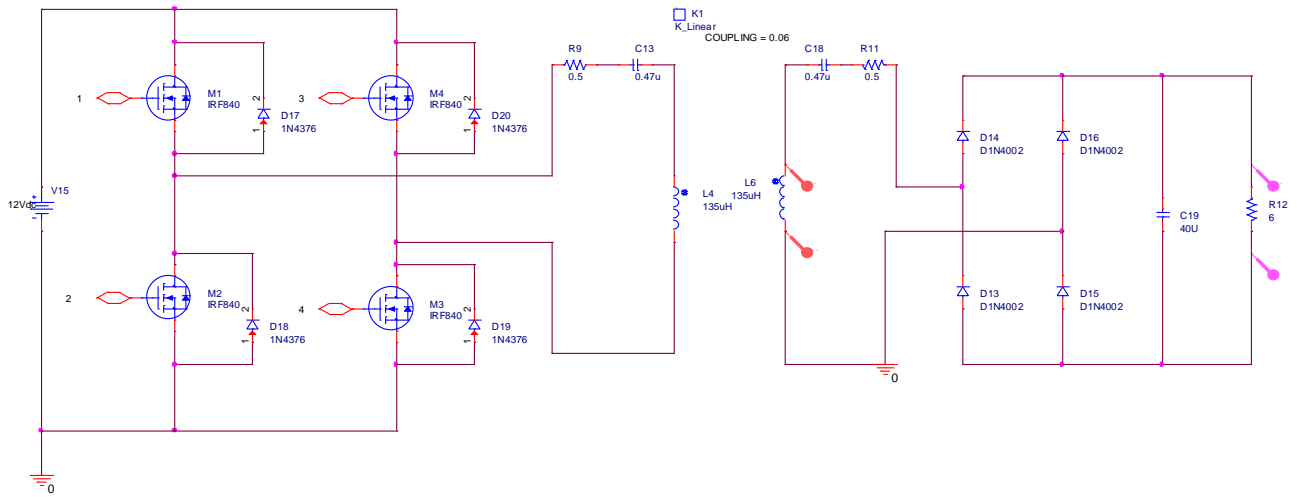

Fig. 7 IR2110 Drive Circuit
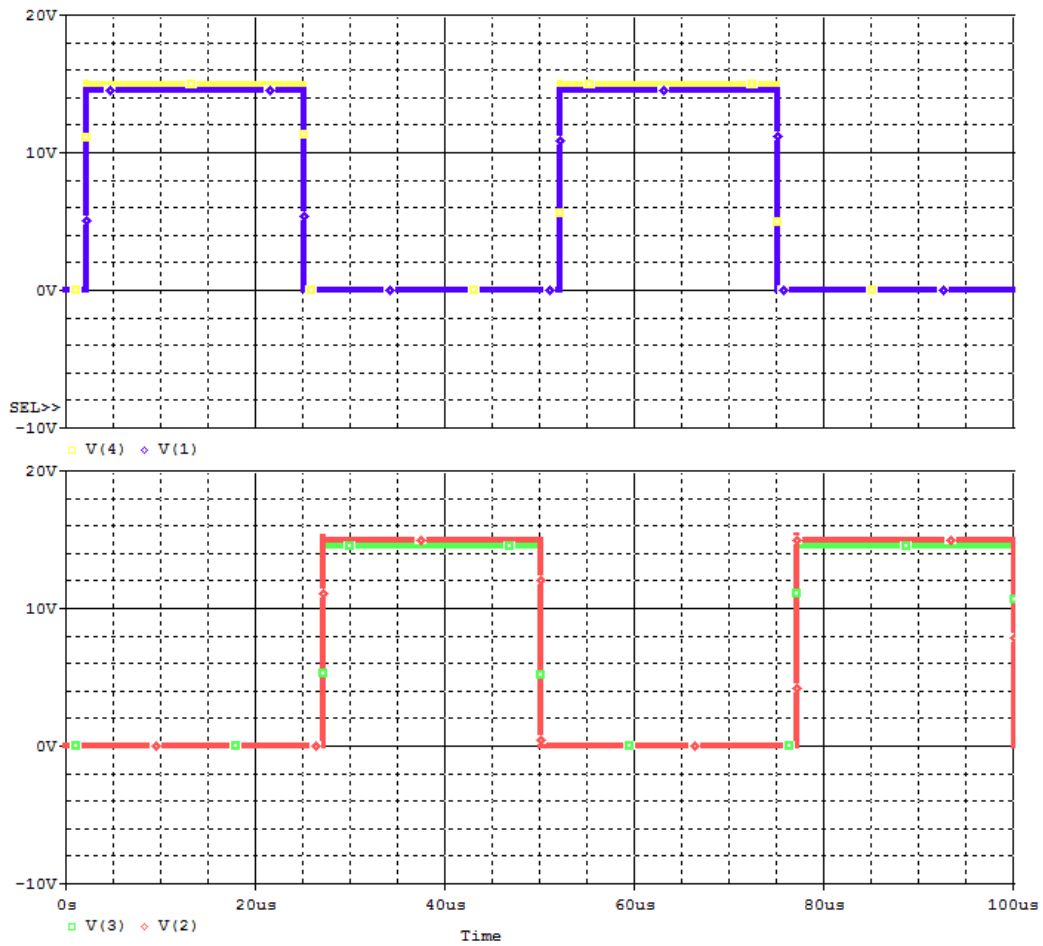
Fig. 8 System Simulation Diagram
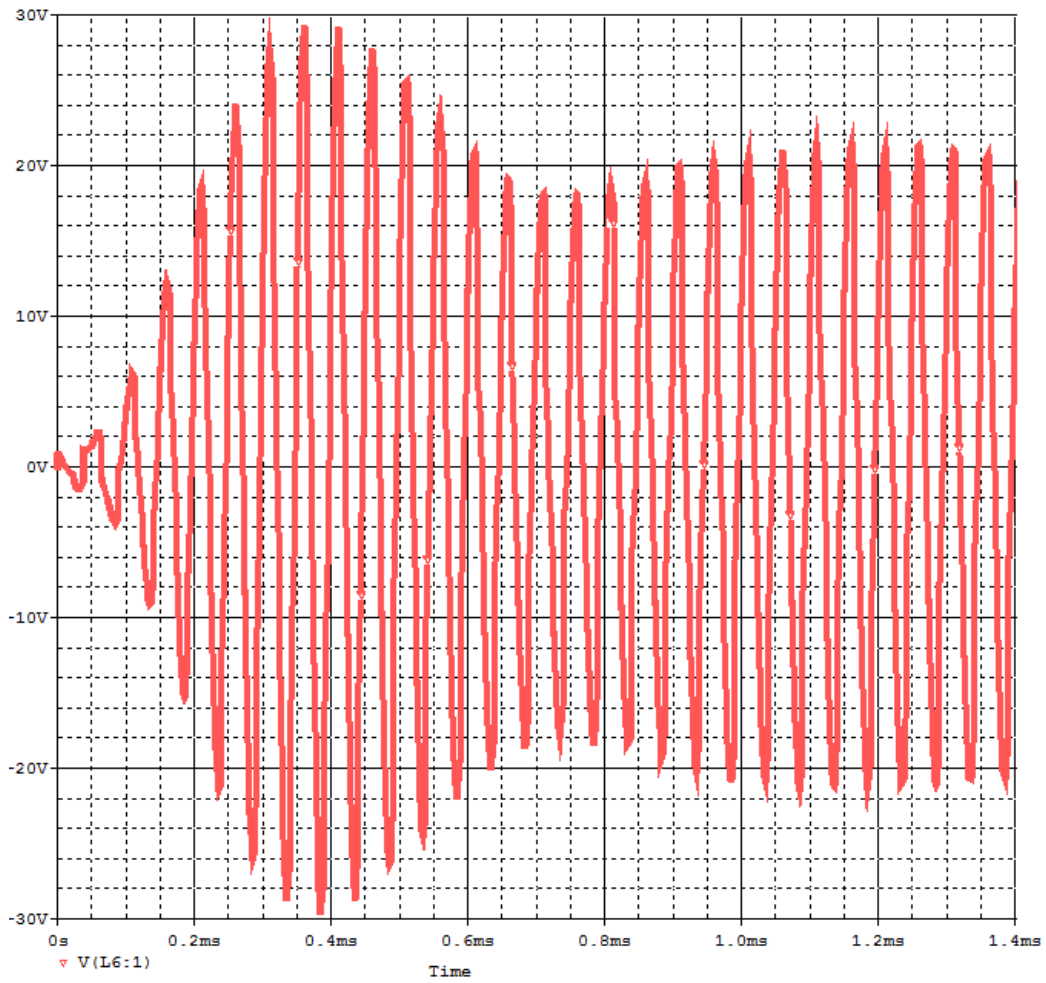

Fig. 9 IR2110 Waveform Diagram
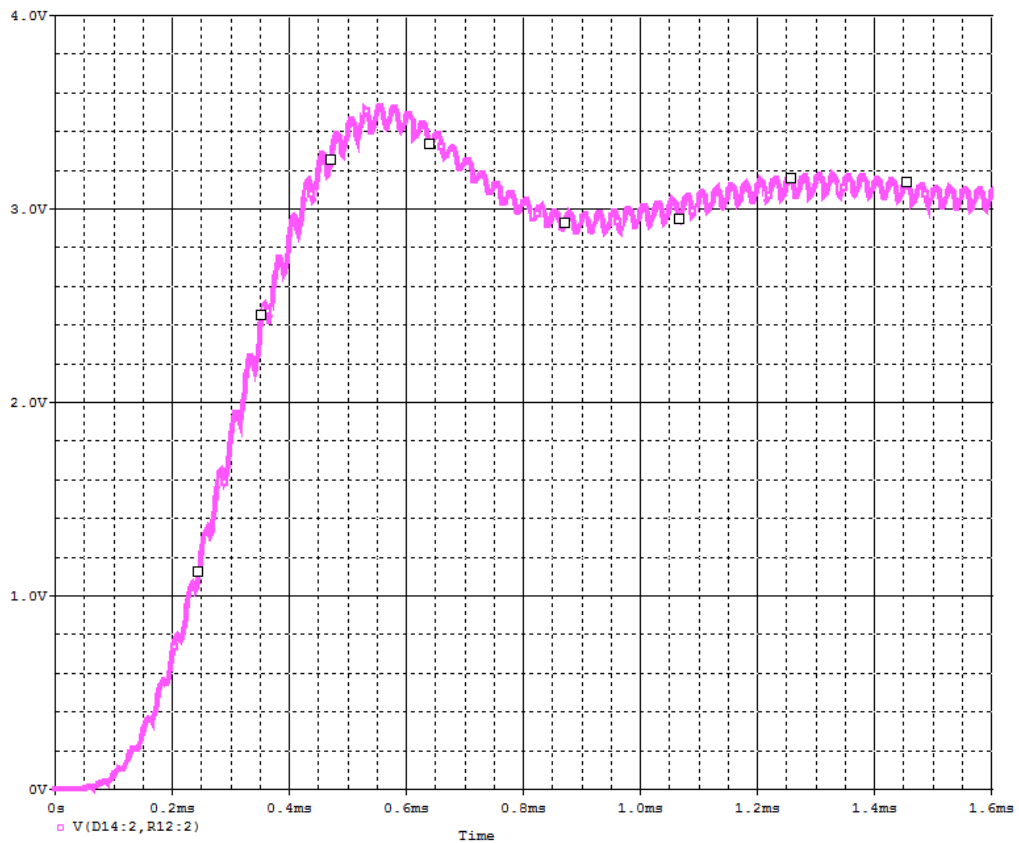
Fig. 10 Secondary Coil Voltage

Fig. 11 Load Voltage

3. Experimental

A RWPT system is designed to verify the validity and feasibility of theoretical analysis and simulation analysis. The system parameters are shown in Table 1, and the components selection is shown in Table 2.

Table 1. System Parameters

Parameter	Value
Voltage/V	12
L_1/μH	135
L_2/μH	135
C_1/μF	0.47
C_2/μF	0.47
Load/Ω	150

Table 2. Component Selection

Component	Model
MOSFET	irf840
Fly-wheel diode	1N4148
Commutation diode	D1N5820
Filter capacitor	4.7uF
Inverter control chip	IR2110
DSP	TMS320F28335

The degree of coupling between the two sides of the coil is smaller and smaller with the increasing of the distance of the coil, and the experiment is based on the different spacing of the coil. The distance between the coils is 2cm, 3cm, 4.5cm, 6cm, 9cm, 12cm, 15cm, 18cm, 9cm.The load range is 0~100Ω.The 6cm distance experiment data is shown in Table 3.

Table 3. Experimental data from 6cm

Load/Ω	Voltage/V	Current/A	Power/W
1.5	2.62	1.27	3.3274
4.4	3.86	1.92	7.4112
8.7	6.15	1.95	11.9925
11.8	6.87	2.05	14.0835
14.5	7.26	2.05	14.883
18.4	8.15	1.92	15.648
24.9	8.17	2.06	16.8302
32.4	8.58	2.01	17.2458
55.3	8.91	2.01	17.9091
70	9.35	2.04	19.074
105.5	9.42	2.06	19.4052

Further, the experimental data from different distances were statistically analyzed. The relationship between load resistance and transmission power under different transmission distances is obtained, as shown in FIG 12.

Analyzing FIG. 12, it shows that the transmission power increases firstly and then decreases with the increase of distance. For this experiment, when the transmission distance is 4.5cm, the transmission power is always maintained at the maximum value of different distances under the same resistance. The above figure shows the trend that the coupling coefficient decreases with the increase of transmission distance. At the same time, the output power increases firstly and then decreases with the increase of coupling coefficient. The experimental results are in agreement with the results of the previous theoretical analysis.
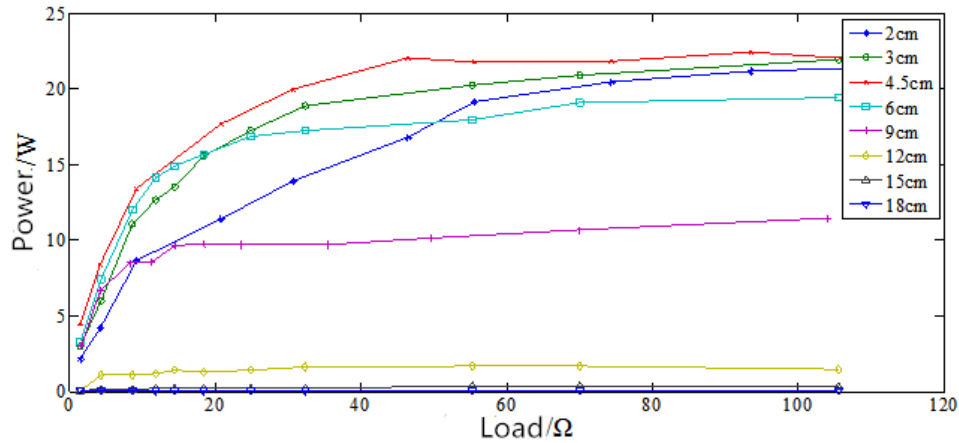
Fig. 12 Relationship between Load Resistance and Transmission Power under Different Transmission Distances

4. Summary

In this study, we studied the characteristics of RWPT in detail, and the relationship between the impedance, frequency and power of the system is analyzed with the help of mathCAD software, and the whole system is analyzed with the aid of PSpice software. Finally, the experimental system is built to investigate the transmission power of the system under the resonance frequency of 20 kHz, and the consistency between the theoretical analysis and the actual experiment is verified. At the same time, it lays the foundation for the next step of battery charging and energy feedback processing.

Acknowledgements

Reference

[1]. Kurs A, Karalis A, Moffatt R, et al. Wireless power transfer via strongly coupled magnetic resonances [J]. Science, 2007, 317 (5834): 83-86.

[2]. Jianliang Li, Jing Kang, Chenglin Tian, et al. Study on Wireless Power Transfer Technology with Series-Series Type of Magnetic Coupling Resonance Model[A]. Proceedings of the 2nd International Conference on Computer Engineering, Information Science and Internet Technology (CII 2017) [C].Wuhan, China, 2017 . 225-232.

[3]. Li Jianliang, Cheng Bo. Study on a Wireless Power Transfer System with the Series-Series Type of Magnetic Coupling Resonance [J]. Journal of Shaoyang University (Natural Science Edition), 2018, 15 (02):46-54(in Chinese).

[4]. 4. Wenxian Chen, Qianhong Chen, Juntao Huang, et al. Analysis and research of distance transmission characteristics of magnetic resonance WPT system [A] . 2014 IEEE VTC [C]. Seoul, Korea, 2014. 1-5.

[5]. V. B. Gore and D. H. Gawali, "Wireless power transfer technology for medical applications," 2016 Conference on Advances in Signal Processing (CASP), Pune, India, 2016, pp. 455-460.